

Article

Contribution of the Tyrosinase (MoTyr) to Melanin Synthesis, Conidiogenesis, Appressorium Development, and Pathogenicity in *Magnaporthe oryzae*

Xiaoning Fan¹, Penghui Zhang¹, Wajjiha Batool¹, Chang Liu¹, Yan Hu¹, Yi Wei¹, Zhengquan He² and Shi-Hong Zhang^{1,*} 

¹ The Key Laboratory for Extreme-Environmental Microbiology, College of Plant Protection, Shenyang Agricultural University, Shenyang 110866, China

² Key Laboratory of Three Gorges Regional Plant Genetics & Germplasm Enhancement (CTGU), Biotechnology Research Center, China Three Gorges University, Yichang 443000, China

* Correspondence: zhangsh89@syau.edu.cn

Abstract: Dihydroxynaphthalene-(DHN) and L-dihydroxyphenylalanine (L-DOPA) are two types of dominant melanin in fungi. Fungal melanins with versatile functions are frequently associated with pathogenicity and stress tolerance. In rice blast fungus, *Magnaporthe oryzae*, DHN melanin is essential to maintain the integrity of the infectious structure, appressoria; but the role of the tyrosinase-derived L-DOPA melanin is still unknown. Here, we have genetically and biologically characterized a tyrosinase gene (*MoTyr*) in *M. oryzae*. *MoTyr* encodes a protein of 719 amino acids that contains the typical CuA and CuB domains of tyrosinase. The deletion mutant of *MoTyr* ($\Delta MoTyr$) was obtained by using a homologous recombination approach. Phenotypic analysis showed that conidiophore stalks and conidia formation was significantly reduced in $\Delta MoTyr$. Under different concentrations of glycerol and PEG, more appressoria collapsed in the mutant strains than in the wild type, suggesting *MoTyr* is associated with the integrity of the appressorium wall. Melanin measurement confirmed that *MoTyr* loss resulted in a significant decrease in melanin synthesis. Accordingly, the loss of *MoTyr* stunted the conidia germination under stress conditions. Importantly, the *MoTyr* deletion affected both infection and pathogenesis stages. These results suggest that *MoTyr*, like DHN pigment synthase, plays a key role in conidiophore stalks formation, appressorium integrity, and pathogenesis of *M. oryzae*, revealing a potential drug target for blast disease control.

Keywords: *MoTyr*; melanin; conidiophore stalks; appressorium; pathogenesis; *Magnaporthe oryzae*



Citation: Fan, X.; Zhang, P.; Batool, W.; Liu, C.; Hu, Y.; Wei, Y.; He, Z.; Zhang, S.-H. Contribution of the Tyrosinase (*MoTyr*) to Melanin Synthesis, Conidiogenesis, Appressorium Development, and Pathogenicity in *Magnaporthe oryzae*. *J. Fungi* **2023**, *9*, 311. <https://doi.org/10.3390/jof9030311>

Academic Editors: Jun Yang, Xiaolin Chen, Haifeng Zhang, Min He and Junjie Xing

Received: 31 January 2023
Revised: 15 February 2023
Accepted: 20 February 2023
Published: 28 February 2023



Copyright: © 2023 by the authors. Licensee MDPI, Basel, Switzerland. This article is an open access article distributed under the terms and conditions of the Creative Commons Attribution (CC BY) license (<https://creativecommons.org/licenses/by/4.0/>).

1. Introduction

Melanin is a unique pigment with myriad functions and is found in various organisms, including fungi. It is produced by specialized cells called melanocytes and is responsible for the coloration of the skin, hair, and other tissues. Melanin plays multifunctional roles in an organism, including protection against environmental stresses such as ultraviolet (UV) radiation, detoxifying harmful substances, and participating in immune responses [1]. In fungi, melanin is thought to play a number of important roles in fungal defense. It protects the fungi against UV radiation and other harsh environments helping them to survive in a wide variety of environments, including on the surface of plants, in soil, and in water. Also, melanin is thought to have antioxidant properties and may help to protect fungi against oxidative stress [2]. In addition to the role of melanin in fungal defense, the substantial protective powers of melanin play decisive roles in the virulence of many fungal pathogens [3,4].

There are two main melanin synthesis pathways in fungi: Dihydroxynaphthalene (DHN) synthesis pathway and L-dihydroxyphenylalanine (L-DOPA) synthesis pathway [5,6]. The first pathway begins with malonyl-CoA as a precursor molecule, followed by a series of

enzymatic modifications that leads to the polymerization of 1,8-DHN to yield DHN melanin. The second pathway begins with tyrosine or L-dopamine and leads to the dihydroxy indoles polymerization, resulting in DOPA melanin [7]. The specific pathway of melanin synthesis can vary depending on the type of fungus and the specific conditions it is experiencing. The DHN melanin resides primarily in ascomycetes and related deuteromycetes [8]. Most plant pathogens use the DHN pathway to synthesize melanin, such as *Magnaporthe oryzae*, *Aureobasidium melanogenum* and *Colletotrichum lagenarium* [9–12]. Alternatively, a few fungi synthesize melanin via the L-DOPA pathway. It is seen mostly in some animals and human pathogenic fungi, such as *Cryptococcus neoformans*, *Candida albicans* and *Histosidium capsulatum* [13–15].

DHN-melanin biosynthesis starts with a polyketide synthase (PKS) using acetyl coenzyme A or malonyl coenzyme A as a precursor to synthesize the polyketide chain following a series of condensation reactions (Supplement Figure S1A). Once the polyketide chain has been synthesized, it is modified through a series of enzymatic reactions, including cyclization, hydroxylation, oxygenase-mediated cleavage, etc., to yield DHN-melanin. The exact sequence of reactions and the enzymes involved can vary depending on the organism in which DHN-melanin is being synthesized [16].

Enzymes involved in melanin synthesis have been studied in many fungi. For example, *Pks1* (encoding polyketide synthase), *Scd1* (encoding scytalone dehydratase), and *Thr1* (encoding trihydroxynaphthalene reductase) have been cloned and characterized in many fungi [10,17–19]. Studies have shown that deleting these genes lead to abnormal melanin synthesis and fungal dysfunction. In *Colletotrichum gloeosporioides*, deletion of the *Pks1* resulted in the failure of the mutants' colony hyphae and appressoria to properly synthesize melanin which leads to the reduced turgor pressure of the pathogen during host attachment [20]. In *Sporothrix schenckii*, the absence of scytalone dehydratase enzyme prevents the production of DHN-melanin, resulting in its loss of dominance under various stresses [21]. In *Setosphaeria turcica*, the absence of *LAC2* (encoding laccase) blocks the development and maturation of the appressoria in mutant strains and thus decreases the pathogenicity of fungus in maize [22]. Similarly, three genes, *ALB1*, *BUF1*, and *RSY1*, were identified to be involved in *M. oryzae* melanin synthesis. These genes are known to be required for conidial resistance and environmental stress tolerance, and their deletion led to a loss of melanin synthesis and virulence in *M. oryzae* [17,23,24].

The L-DOPA pathway is another pathway for melanin synthesis in fungi. It is less common than the DHN pathway in fungi, but it is the dominant pathway for melanin synthesis in animals, including humans [25]. There are two precursor substances in the L-DOPA melanin synthesis pathway: tyrosine and dopamine. Tyrosinase (EC 1.14.18.1) is the main rate-limiting enzyme in this synthetic pathway, which is primarily involved in two reactions: catalyzing the conversion of L-tyrosine to L-dopamine and subsequent oxidation of L-dopamine to form dopamine quinone, which undergoes a series of reactions to form melanin (Supplement Figure S1B) [26]. Current studies on fungal tyrosinases have mainly focused on enzyme crystal structure, its enzymatic activity and inhibitors [27–31]. For example, the tyrosinase gene from *Aspergillus oryzae* was cloned and expressed to achieve its application in L-DOPA biotransformation [32]. In *Armillaria ostoyae*, replacing D262 with asparagine significantly increased the catalytic efficiency of monophenolase/diphenolase [33]. However, the role of tyrosinase in fungal pathogenicity is not well understood. In *C. neoformans*, the production of L-DOPA melanin catalyzed by tyrosinase is associated with the virulence of pigmented cells. Pigmented cells of *C. neoformans* were found to be less susceptible to free radical killing and amphotericin B, a commonly used antifungal drug. They were more resistant to macrophages, which are cells of the immune system that help to protect the body from infection [34]. Overall, both DHN and L-DOPA melanin pathways are involved in fungal melanin synthesis, and melanin has been shown to play a key role in fungal pathogenesis.

Rice blast caused by *M. oryzae* is the most important and devastating fungal disease on rice, seriously affecting crop yield. The occurrence of rice blasts in a large area is

mainly dependent on its infection cycle. In contrast, the normal development of appressorium, a specialized infection structure formed by *M. oryzae*, plays an important role in the pathogenicity of the rice blast fungus. The mature appressorium cell wall forms a layer of melanin that prevents glycerin and other macromolecular material leakage and plays an important role in maintaining appressorium turgor. [35]. In previous reports, the DHN melanin layer is reported as an impermeable barrier necessary for the host attachment that produces very high dilation pressure, helping the fungus to breach the plant's cell walls and enter the plant's tissues, which is necessary for the disease progression of *M. oryzae* [36]. However, the biological characteristics and pathogenic mechanism of tyrosinase, involved in the L-DOPA melanin pathway in *M. oryzae*, have not been reported yet. In this study, we have identified and functionally evaluated a tyrosinase gene in *M. oryzae* (named *MoTyr*) to determine its role in fungal development and pathogenesis.

2. Materials and Methods

2.1. Sequence Alignment Assays

The *MoTyr* (MGG_14598) gene amino acid sequences were acquired from the NCBI database (<https://www.ncbi.nlm.nih.gov/>, accessed on 2 August 2021). The tertiary structure of *MoTyr* protein was predicted by I-TASSER (<https://zhanggroup.org/I-TASSER/>, accessed on 11 October 2021). Amino acid sequences containing tyrosinase domains identified from other fungi were obtained from the NCBI database, Pfam domain prediction tool was used to predict tyrosinase domains (<http://pfam.xfam.org/search/sequence>, accessed on 11 October 2021). In addition, MEGAX software was used to draw a phylogenetic tree for the conserved domains.

2.2. Fungal Strains and Culture Conditions

M. oryzae strain (Y34) was used in this study. All fungal strains were cultured on complete growth medium {CM (10 g/L glucose, 2 g/L peptone, 1 g/L yeast extract, 1 g/L casamino acids, 0.5 g/L MgSO₄, 6 g/L NaNO₃, 0.5 g/L KCl, and 1.5 g/L KH₂PO₄). In the sporulation test, the RBM (rice bran medium) was used, and mycelium blocks were inoculated onto the RBM, cultured at 28 °C for 7 days in the dark, then scraped off, and cultured under light for 3 days.

2.3. Protoplast Preparation

Protoplasts were prepared for transformation. The wild-type strain was inoculated in CM liquid medium at 28 °C and shaken at 90 r/min for 3–4 days in the dark. The medium was filtered out, and the hyphae were fully ground in a sterile mortar, then added to the fresh CM liquid medium (containing 100 µg/mL streptomycin sulfate) and cultured in a 28 °C shaker for 90 r/min for 12–14 h. Then filtered with sterile paper and washed twice with sterilized ddH₂O (containing 100 µg/mL streptomycin sulfate) and 1 M sorbitol (containing 100 µg/mL streptomycin sulfate). Dried the mycelium and added 40 mL lysing enzyme solution, and incubated in a 30.5 °C shaker for 2–3 h. After that, the completely lysed solution was filtered using a sterile Mira cloth and centrifuged at 5000 rpm for 10 min at 4 °C. Removed the supernatant and added 30–40 mL of Sorbitol STC, then centrifuged at 5000 rpm for 10 min at 4 °C [37].

Finally, the supernatant was removed again and added Sorbitol STC solution. DMSO was added (final concentration was 7%), the protoplast concentration was adjusted to 1×10^6 /mL, and the protoplast was separated into 300 µL volume in a 1.5 mL sterilized centrifuge tube and stored at –80 °C.

2.4. Targeted Gene Deletion of *MoTyr* Mutants

To generate the *MoTyr* deletion strain $\Delta MoTyr$, the *MoTyr* gene was replaced by the hygromycin-resistant cassette (HPH). The primers of *MoTyr*-A-F/R and *MoTyr*-B-F/R (Table S1) were used to amplify Y34 genomic DNA, and the upstream 862 bp (A) and downstream 849 bp (B) sequences of the *MoTyr* gene were obtained, respectively. Fragment

A was fused to the pCX62 vector (after digestion with *EcoR* I and *Kpn* I), and fragment B was fused to the pCX62 vector (after digestion with *BamH* I and *Xba* I) [38]. The primers (MoTyr-A-F and HY/R; YG/F and MoTyr-B-R) amplified hygromycin overlapping fragments, respectively. For transformation, targeted gene deletion using a homologous recombination approach was used as described [39]. Then, MoTyr-ORF-F/R and UAH primers were used to verify the knockout transformants. The primers for gene deletion are listed in Supplementary Table S1.

2.5. Assays for Conidial Production, Growth, and Development

The strains (wild-type and Δ MoTyr) were cultured on RBM media at 28 °C for 7 days in the dark, then removed the hyphae and a sterile blade was used to cut out a medium and placed on a glass slide. The prepared sample was then observed under a Nikon Eclipse 80i microscope at 12, 24, 48, and 72 h. At 72 h, mycelia and conidiophore stalks were stained with lactophenol cotton blue [40]. Conidia in RBM medium were collected by adding 2 mL sterile water, and the numbers were counted under the microscope. Three biological experiments were conducted for each strain, and each experiment was repeated three times.

Conidia of the wild-type and Δ MoTyr were cultured on RBM media and collected to observe the germination of conidia and formation of appressoria. The conidial suspension was adjusted to 1×10^5 /mL and added dropwise to a hydrophobic cover slip under a microscope at 2, 4, and 6 h. Wild type and mutant spores were exposed to -20 °C and UV for 12 h and 30 min, respectively, and observe the germination of spores. Three biological experiments were conducted for each strain, and each experiment was repeated three times.

2.6. Analysis for Appressorium Integrity

In order to test the effect of MoTyr on the integrity of the appressorium wall and turgor pressure generated by it, 50 μ L of spore suspension with a concentration of 5×10^4 conidia/mL was dropped onto the surface of the hydrophobic membrane and incubated at 28 °C for 24 h. After the appressorium was generated, the water layer covering the spore was carefully removed. It was treated with 50 μ L glycerol solution with concentrations of 1 M, 2 M, 3 M and 4 M, respectively, and kept wet at 28 °C for 10 min. The appressorium collapse was observed under a microscope and recorded [41].

Under the same experimental conditions, 20%, 25%, 30% and 35% PEG3350 solution instead of glycerol was used to treat the appressorium, and the collapse of appressoria cells was observed by microscope. Each strain of the above experiments was used to observe the appressoria isolated from the plasma wall, and the appressoria number was at least 100. The experiment was repeated 3 times.

2.7. Rice Sheath Penetration and Plant Infection Assays

To test the pathogenicity of the MoTyr, the wild-type and Δ MoTyr were cultured on RBM and collected conidia as previously described. At the four-leaf stage of rice seedlings (*Oryza sativa* cv. Lijiangxintuanheigu), the 1 mL spore suspension (1×10^5 conidia/mL in 0.25% gelatin) was inoculated on the surface of rice leaves and incubated in the dark for 24 h in a culture chamber at 28 °C, then changed to a photoperiod of 16 h for 7 days. For the infection test of barley leaves, 20 μ L spore suspension was inoculated on intact and injured barley leaves and cultured under similar conditions as described above.

The spore suspension (1×10^5 conidia/mL) was injected into the leaf sheath of rice and then put in a moist environment. The infection rates of leaf sheaths and the types of infectious hyphae (IH) at 12, 24 and 48 h post-inoculation (hpi) were analyzed and repeated in triplicate as previously described. The experiment performed three biological replicates.

2.8. Extraction and Purification of Melanin

To determine the melanin content of the wild-type and Δ MoTyr, collected conidia suspensions (1×10^5 conidia/mL) were cultured at 28 °C for 24 h for appressoria production. Centrifuged at 5000 rpm for 10 min, the supernatant was dumped, the precipitate

was dried and weighed, and 1 mL of 1 M NaOH was added (according to 1:120 (*w/v*)). Continue heating at 121 °C for 20 min to extract melanin; after extraction, the supernatant was filtered, and the volume was fixed to 1 mL, with 1 M NaOH as a blank control. The absorbance value was measured at 405 nm.

2.9. Statistical Analysis

All the experiments were performed at least three times. SPSS Statistics 25 was used for data statistics and analysis. The analysis was performed using an independent samples t-test. Error bars represent the standard deviation. * indicates a statistically significant difference at $p < 0.05$. ** indicates a highly significant difference at $p < 0.01$.

3. Results

3.1. MGG_14598 Encodes a Tyrosinase in *M. oryzae*

Tyrosinase exists in many species, and its functional mechanisms have been reported in many species [33,42–44]. At present, the mechanism of tyrosinase action in blast fungus is not clear.

A putative tyrosinase, MGG_14598, was identified in the *M. oryzae* genome that encodes a putative tyrosinase protein and contains a common central domain of tyrosinase in *M. oryzae*. Hence, the gene was named *MoTyr*, with a 2160 bp open reading frame length, encoding a protein of 719 amino acids. Tyrosinase is present in many fungi. We compared the relationship between tyrosinase proteins of six fungi and *M. oryzae* *MoTyr*. *MoTyr* was closely related to tyrosinase in *Neurospora crassa* (Figure 1A). *MoTyr* protein structure has an important domain: the Tyrosinase domain (79–322) (Figure 1B), and has two copper coordination sites, CuA (83–122) and CuB (277–315), and six conserved histidine residues that are involved in the coordination between the two copper sites [45,46]. Consistent with our results, alignment comparison and 3D structure revealed that *MoTyr* protein had conserved histidine residues with *A. ostoyae* and *Colletotrichum spinosum* at residues H88, H112, H121, H283, H287 and H310 (H88, H112, H283 for CuA and H283, H287, H310 for CuB; Figure 1B,C). These results indicate that domains of tyrosinase are well conserved in the fungal group.

To further evaluate the biological characteristics of the *MoTyr* gene, we analyzed the expression abundance of *MoTyr* at different developmental stages of *M. oryzae*. We found that the expression of *MoTyr* was downregulated on the 5th and 6th day of mycelia growth. On the 7th day of development, the mycelium was removed and developed into conidiophore stalks. However, the expression of *MoTyr* was up-regulated in the conidiophore stalks during 6–12 h of development. The expression of this gene began to be downregulated in the later stages of development (Figure 1D). In addition, we injected wild-type spore suspensions into rice leaf sheaths and examined the expression of *MoTyr* at different infection stages. The results showed that *MoTyr* was highly expressed at the early stage of infection (12 and 24 hpi) but was downregulated at 36 hpi of infection (Figure 1E). These results suggest that *MoTyr* may be involved in conidiophore stalks development and may play a key role in the early stage of infection.

3.2. *MoTyr* Is Important for Conidiophore Stalks and Conidiation Development

The expression of *MoTyr* was high during the development of the conidiophore stalks of *M. oryzae*, so we speculated that *MoTyr* might be involved in the development of the conidiophore stalks. To prove our hypothesis, we deployed a homologous recombination approach for targeted gene deletion of the *MoTyr* gene using the pCX62 vector. Two *MoTyr* gene deletion strains ($\Delta MoTyr-10$, $\Delta MoTyr-31$) were successfully obtained and further confirmed through PCR (Supplement Figure S2A,B).

We shaved off the hyphae on RBM, and a piece of the culture medium was cut with a sterile blade and cultured at 28 °C and observed the development state of conidiophore stalks at 12, 24, 48 and 72 h under a microscope. The results showed that the development of conidiophore stalks of the mutants was slower, and the development of

mycelia was sparse compared with that of the wild-type at the same development time (Figure 2A). We used lactophenol cotton blue to stain the conidiophore stalks, and the results showed that the number of conidiophore stalks in the mutant was significantly lower than wild-type (Figure 2B).

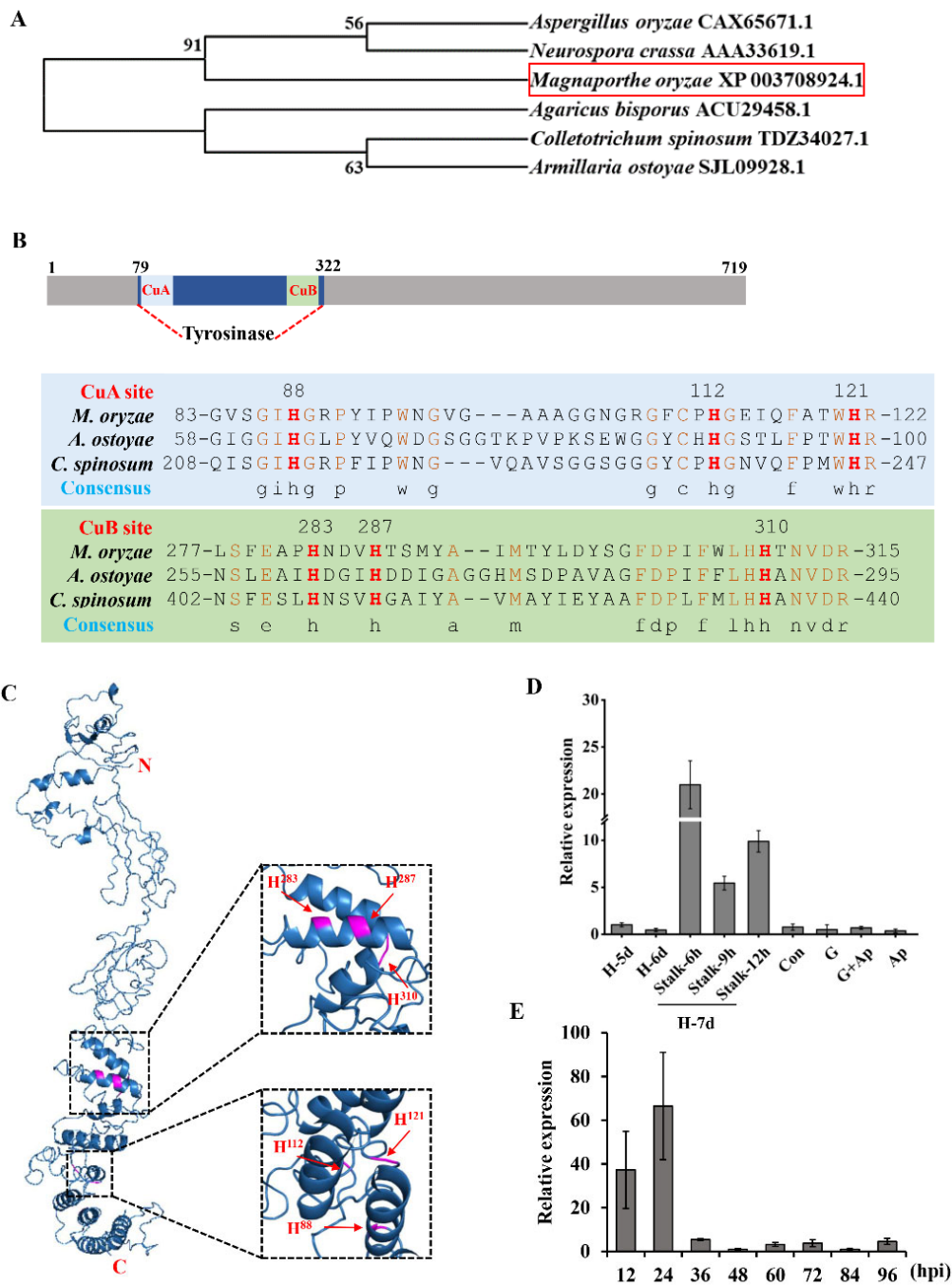


Figure 1. Phylogenetic analysis, protein structure, domain alignment, and expression of tyrosinase MoTyr in *M. oryzae*. (A) Phylogenetic tree constructed with tyrosinase homologs from *M. oryzae*, *A. oryzae*, *N. crassa*, *A. bisporus*, *C. spinosum*, and *A. ostoyae*. (B) Amino acid sequence alignment of tyrosinases from *M. oryzae*, *A. ostoyae*, and *C. spinosum*. Histidine residues participating in copper coordination are marked in bold red font. (C) Tertiary structure (3-D) of MoTyr. (D) Expression level of MoTyr in *M. oryzae* at different developmental stages. (E) Expression level of MoTyr in leaf sheath infected at different periods in wild-type. H, hyphae; Stalk, conidiophore stalks; Co, conidia; G, germ tube; Ap, appressoria.

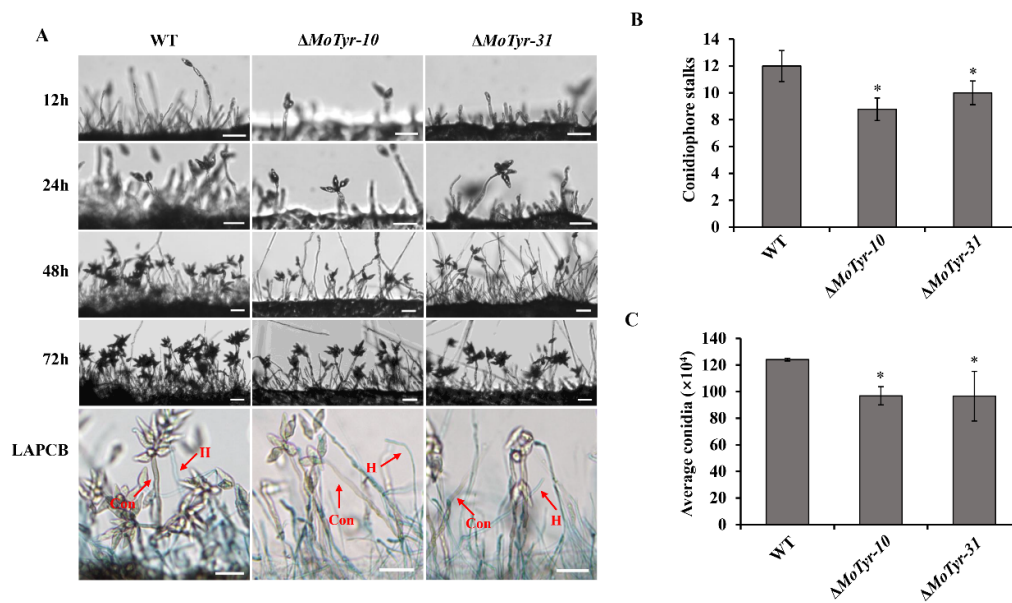


Figure 2. Conidiophore stalks and conidiation development of wild-type and $\Delta MoTyr$ mutant strains. (A) The conidiophore stalks of the wild-type and $\Delta MoTyr$ strains were induced for 12, 24, 48, and 72 h; strains were stained with lactophenol cotton blue at 72 h. The hyphae were stained blue, whereas the conidiophore stalks and conidia were grey; Scale bar = 20 μ m; LACPCB, Lactophenol cotton blue; H, hyphae; Con, conidiophore stalks. (B) Statistical analysis of conidiophore stalks in wild-type and $\Delta MoTyr$ strains. (C) Conidia count in wild-type and $\Delta MoTyr$ strains. Asterisks * represent a statistically significant difference of $p < 0.05$. Error bars indicate the mean \pm SD from three independent experiments.

The conidiation may be affected by the obstruction of conidiophore stalks formation. We examined the conidial production of the mutants and wild-type and found that the spores produced by the knockout mutant $\Delta MoTyr$ were significantly reduced than that of the wild-type (Figure 2C). The normal development of conidia and appressorium is an important factor in the pathogenicity of *M. oryzae*. The results showed that deleting *MoTyr* did not affect mutants' vegetative growth and normal spore morphology development (Supplement Figure S3). In addition, the spore germination and appressorium formation of the *MoTyr* deletion mutants were not significantly different from the wild-type (Supplement Figure S4). Our results show that the deletion of *MoTyr* has not affected the conidial germination and appressorium morphogenesis, but it has reduced the number of conidiophore stalks and spores, which indicates that *MoTyr* is important for conidiophore stalks and conidiation formation.

3.3. *MoTyr* Is Essential for the *M. oryzae* Appressoria Integrity

Tyrosinase is a rate-limiting enzyme involved in melanin synthesis. The appressorium of *M. oryzae* is the key factor in infecting the host plant, and the normal formation of melanin plays an important role in maintaining the appressorium function of *M. oryzae*. We test the effect of deletion of the *MoTyr* gene on the cell wall integrity of the appressorium of *M. oryzae*, the appressoria formed by wild-type and mutant strains on the hydrophobic membrane were treated with glycerol and PEG solution. Our results showed that cell collapse occurred in all strains after the appressoria were treated with glycerol at different concentrations. The degree of appressoria collapse of $\Delta MoTyr$ was stronger than that of the wild-type under the treatment of 1 M, 2 M and 3 M of glycerol (Figure 3A,B). The appressoria collapse rate of $\Delta MoTyr-10/\Delta MoTyr-31$ was 1.58/1.54, 1.43/1.72, and 1.10/1.24 times that of the wild-type at 1 M, 2 M and 3 M concentrations of glycerol, respectively. However, there was no significant difference in the collapse rate between the mutants and wild-type under the treatment of 4 M of glycerol, indicating that the concentration of glycerol had

reached the maximum tolerance of the appressoria (Figure 3B). At the same time, the appressoria collapsed after treatment with different concentrations of PEG solution, and the appressoria collapse rate of the *MoTyr* deletion strains was significantly higher than that of the wild-type (Figure 3C,D). These results suggest that *MoTyr* is important for the cell wall integrity of the appressorium.

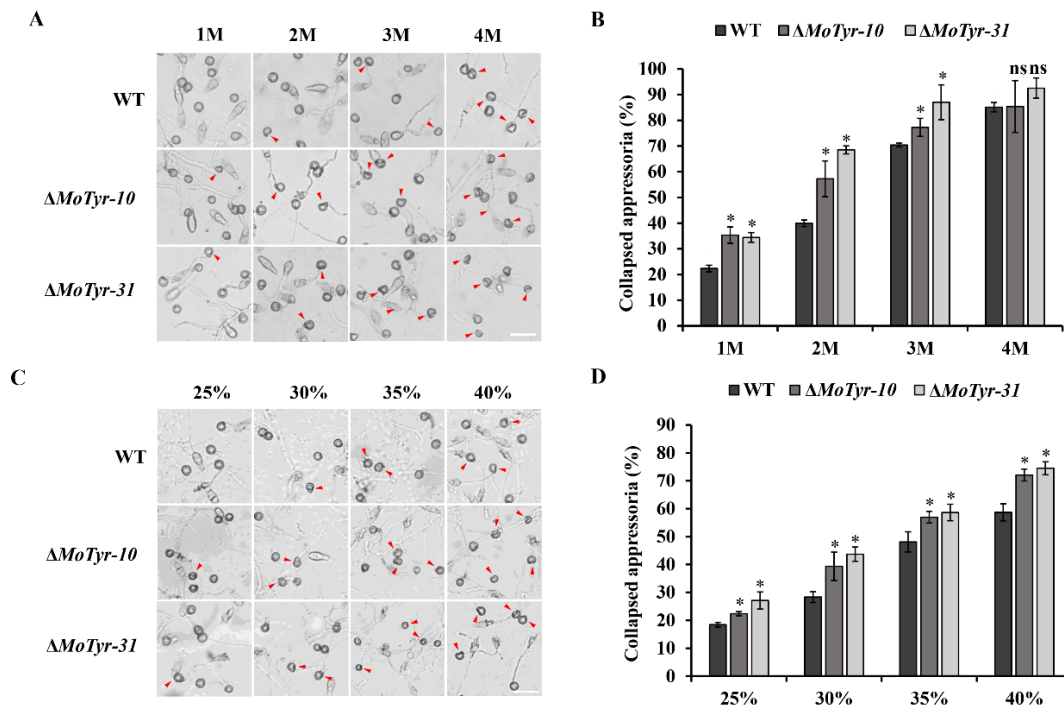


Figure 3. Appressoria development analysis of the wild-type and $\Delta MoTyr$ mutant strains. (A) Cytorrhysis assay for appressorium turgor pressure determination. Conidia (1×10^5 conidia/mL) of wild-type and mutant strains were seeded on hydrophobic mulch, and appressoria produced after 24 h of dark culture at 28 °C were treated with different concentrations (1, 2, 3, and 4 M) of glycerol; The red arrow pointed to the collapsed appressorium; Scale bar = 20 μ m. (B) A statistical representation of proportion-collapsed appressoria recorded for the individual strains under the different concentration glycerol solutions treatments. (C) Appressorium turgor pressure determination was treated with different concentrations (25%, 30%, 35%, and 40%) of PEG; The red arrow pointed to the collapsed appressorium; Scale bar = 20 μ m. (D) A statistical representation of proportion-collapsed appressorium recorded for the individual strains under the different concentration PEG treatments. For each biological replicate of Figure A and C, a total of 100 appressoria were counted ($n = 100 \times 3$). Asterisks * represent a statistically significant difference of $p < 0.05$; ns represent not significant.

3.4. *MoTyr* Loss Affected Melanin Synthesis and Stress Resistance in *M. oryzae*

Appressorium turgor is generated by the rapid influx of water into the cell against a concentration gradient of glycerol that is maintained in the appressorium by a specialized, melanin-rich cell wall. The normal synthesis of melanin plays an important role in maintaining appressorium turgor. In our study, we tested tyrosinase activity in the hyphae of the mutant and wild-type and found that the tyrosinase activity in the mutant was significantly lower than that of the wild-type (Figure 4A). The results showed that the *MoTyr* gene is involved in the synthesis of tyrosinase. Tyrosinase is an important rate-limiting enzyme in the L-DOPA melanin synthesis pathway, but whether the deletion of this gene will affect melanin synthesis in *M. oryzae* is unknown. We tested melanin levels in both mutants and wild-type; the marginal hyphae of mutant and wild-type were inoculated into CM liquid medium after 7 days of shock culture at 28 °C and found that the blackening level of the mutants was weaker than that of the wild-type (Figure 4B). In addition, compared to the variation of melanin content in conidia and appressoria, the results showed that the

melanin content in the mutant strains was significantly lower than that of the wild-type (Figure 4C). These results suggest that MoTyr is involved in melanin synthesis and plays an important role in the appressorium development of *M. oryzae*.

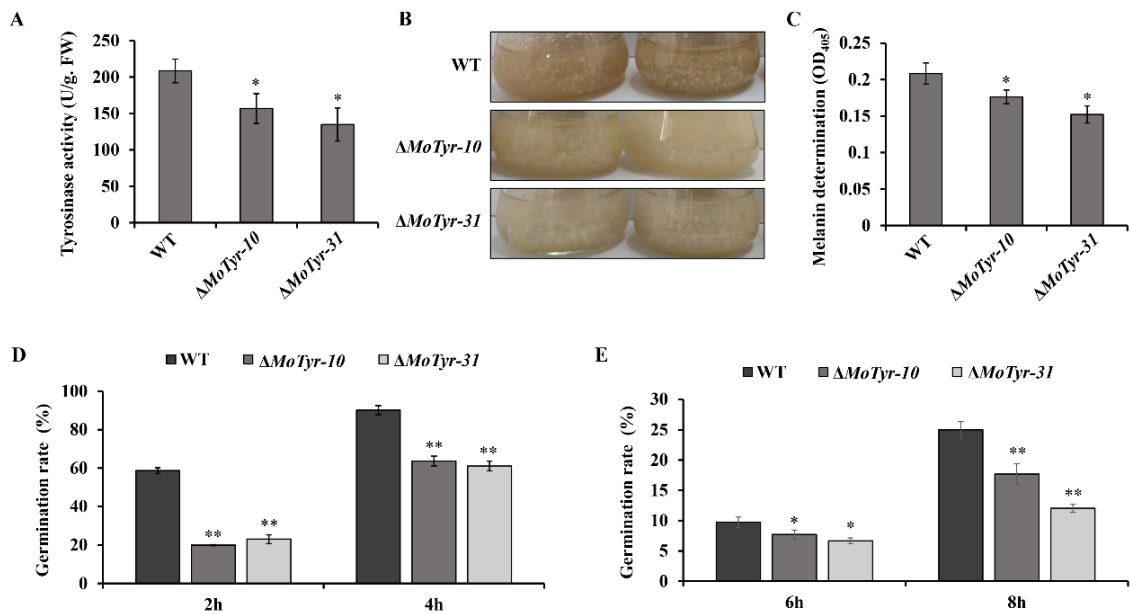


Figure 4. Detection of melanin levels in mutant strains and conidial germination of *M. oryzae* spores under environmental stresses. (A) Detection of tyrosinase activity in hyphae of mutants and wild-type. (B) Melanin was decreased in the $\Delta MoTyr$ mutant strains. (C) The melanin content of strains in conidia and appressoria. (D) Germination rate of conidia at $-20^{\circ}C$ for 12 h. (E) Germination rate of conidia exposure to UV for 30 min. The analysis was performed using an independent samples t-test. Note: Statistical analyses were performed with data obtained from three biological replications with three technical replicates each time. Asterisks * represent a statistically significant difference of $p < 0.05$, and ** represent a statistically significant difference of $p < 0.01$.

In fungi, normal synthesis of melanin favors increased fungal tolerance to abiotic and biological environmental stresses, including radiation, extreme temperatures, dryness, metal toxicity, and host immune responses [47–49]. We examined the spore germination of the MoTyr deletion mutant under stress conditions. After freezing at $-20^{\circ}C$ for 24 h, the conidial germination rates of the $\Delta MoTyr$ at different times were significantly lower than those of the wild-type (Figure 4D). After exposure to UV for 30 min, the conidial germination rate of $\Delta MoTyr$ strains was significantly lower than that of the wild-type (Figure 4E). These results suggest that the deletion of MoTyr inhibits melanin synthesis, thereby reducing the ability of *M. oryzae* to resist abiotic and biological environmental stresses.

3.5. MoTyr Is Important for Pathogenicity in *M. oryzae*

In order to detect the role of MoTyr in the pathogenic development of *M. oryzae*, we collected conidia from wild-type and $\Delta MoTyr$ strains and tested them for pathogenicity. When intact susceptible rice seedlings were spray-inoculated with conidial suspension, we found that the rice leaves inoculated with mutant spores were less susceptible to the disease and had lower disease incidence than those inoculated with wild-type (Figure 5A). Similarly, when drop-inoculation was assayed, the mutant strains still showed weaker pathogenicity than the wild-type (Figure 5B). In addition, we treated the intact and injured barley leaves with wild-type and $\Delta MoTyr$ hyphae and found that under intact treatment, the disease lesions on mutant strains' inoculated barley leaves were smaller than wild-type (Figure 5C), but on injured leaves, the degree of disease was similar to that of the wild-type (Figure 5D). These results suggest that MoTyr plays an important role in pathogenesis, and

it may be that the loss of MoTyr resulted in decreased infection ability of appressorium and thus reduced its pathogenic capability.

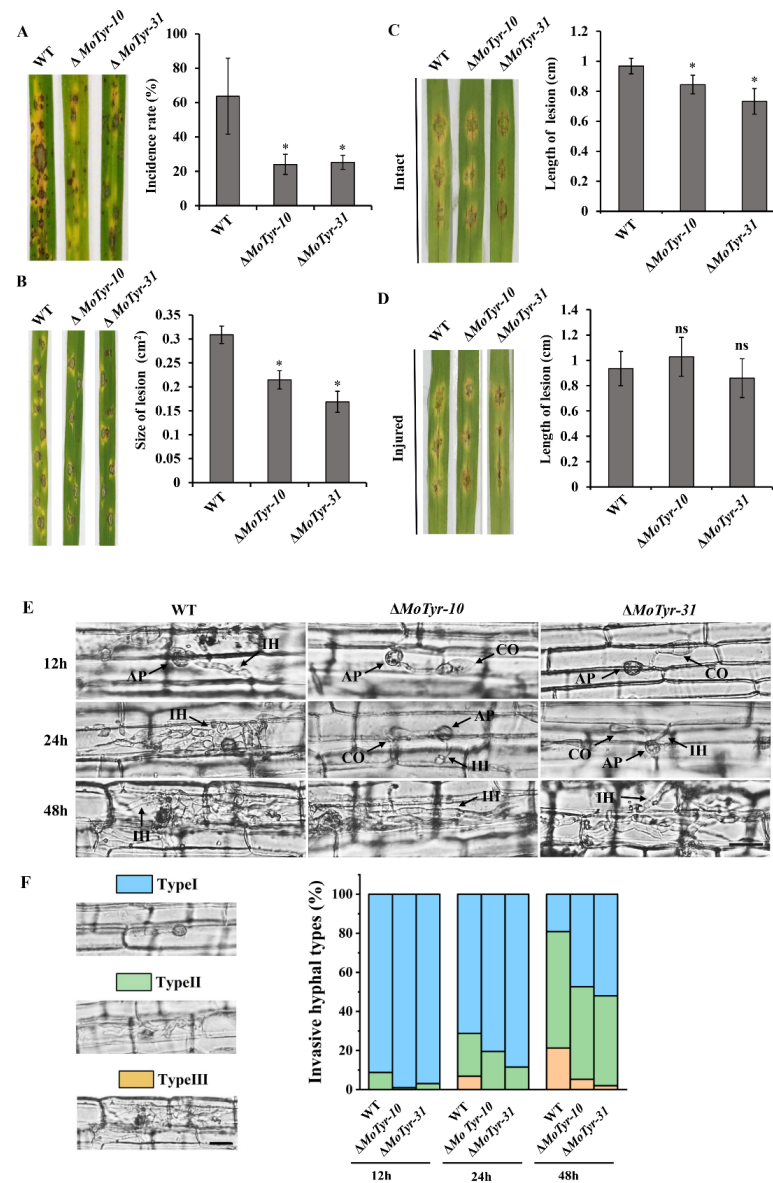


Figure 5. Pathogenesis analysis of the wild-type and mutant strains. **(A)** Spray-inoculation assay. Disease symptoms at 5 dpi of leaves by spraying with conidia (1×10^5 /mL). The graph shows the statistics of the incidence rate of rice leaves. **(B)** Drop-inoculation on leaves. Disease symptoms following the inoculation of rice leaves with 10-mL droplets of conidia (1×10^5 /mL). Representative leaves were photographed at 5 dpi. The graph shows the statistics of lesion size. **(C,D)** Represent the hyphae-mediated blast lesions on intact and injured barley leaves inoculated with mycelial plugs from the wild-type and $\Delta MoTyr$ mutant strains. The graph showed the statistics of the length of the lesion on the barley leaves. **(E)** Rice leaf sheath infection assay. The spore suspensions of wild-type and mutant strains were injected into rice leaf sheaths and cultured at 28 °C. The infection of rice leaf sheaths was observed for 12 h, 24 h and 48 h. The representative infection types were photographed. IH, infectious hyphae, AP, appressoria and CO, Conidia; Scale bar = 10 μ m. **(F)** Statistics of different infection types. Type I: mature appressoria; Type II: formed primary hyphae and invasive hyphae extended and branched in one cell; Type III: invasive hyphae crossing to neighboring cells. Error bars indicate the mean \pm SD from three independent experiments. ns represents not significant, and asterisks * represent a statistically significant difference of $p < 0.05$.

The collapse of the appressorium would result in the weak infection ability and hyphal development of *M. oryzae* in host cells. Therefore, we conducted a microscopic observation of rice leaf sheaths infected by conidia. At 12 hpi, many mature (black) appressorium were formed in both the wild-type and the mutant, but appressorium formation in the mutant was less than in the wild-type. After inoculation for 24 h, the wild-type infected mycelia could develop normally in rice cells and spread to the whole cell. Still, the primary infectious hyphae were just formed in $\Delta MoTyr$. At 48 hpi, the wild-type infected mycelium had begun to spread to neighboring cells, and the mutants had also spread to the entire cell (Figure 5E). In order to quantitatively compare the infection of rice leaf sheath cells by different strains, we divided the infection types into three categories (Type I: mature appressoria; Type II: formed primary hyphae and invasive hyphae extended and branched in one cell; Type III: invasive hyphae crossing to neighboring cells) and analyzed different infection types of more than 50 germinated conidia after inoculation. At 12 hpi, about 8.81% of invasive and primary hyphae had formed in the wild-type, whereas only 0.97% and 3.10% of invasive and primary hyphae formed in the two mutants, respectively (Figure 5F). At 24 hpi, the wild type had formed type III infective hyphae, which can expand to adjacent cells; However, in the mutants, hyphae only developed to type II. At 48 hpi, in the wild type, the infection hyphae formation rate of type III had reached about 21%; At this time, the mutant also formed type III hyphae, but the formation rate only reached 5.26% and 2.00%, respectively (Figure 5F). These results indicated that MoTyr plays an important role in maintaining the infectious development of *M. oryzae*.

4. Discussion

Melanins are insoluble pigments that contribute to microorganism survival, colorization, and UV protection and are also related to fungal virulence in plant and human hosts [25,47]. Melanin has two main synthesis pathways in fungi: the DHN and L-DOPA pathways [5,6]. Various studies have been done on DHN pathway-related enzymes, and their role in pathogens' development and virulence [10,17–24]; however, the L-DOPA pathway has yet to be studied in detail, especially in fungal pathogens. Tyrosinase is the main rate-limiting enzyme involved in the synthesis of L-DOPA melanin, which widely exists in animals, plants, microorganisms, and the human body [32,44,50,51]. In recent years, the research on tyrosinase mainly focuses on medicine, beauty, food and other fields, but there are no relevant studies on tyrosinase in pathogenic fungi.

Rice blast, caused by pathogenic fungi *M. oryzae*, is an important fungal disease of rice [52,53]. It has been reported that the loss of rice yield caused by *M. oryzae* is enough to feed 60 million people every year [54]. Fungal melanin is considered an important virulence factor in a number of fungal species, acting as non-specific armor during infection that protects the fungus against the host immune system [55,56]. In *C. neoformans*, the production of L-DOPA melanin is related to the toxicity of pigmentation cells [34]. Tyrosinase is involved in the L-DOPA melanin synthesis pathway, but its role in the pathogenesis of *M. oryzae* remains unknown. Here, we identified and deployed cell biology, functional genetics, and biochemical techniques to functionally evaluate the contribution of the uncharacterized gene (MGG_14598) named tyrosinase (MoTyr) in morphological and pathogenic development of the economically destructive rice blast fungus. Tyrosinase orthologs are well-conserved in many fungi [32,33]. Our study showed that MGG_14598 encoded protein and all the fungal tyrosinase proteins characterized so far share a conserved tyrosinase domain, two copper coordination sites, CuA and CuB and six conserved histidine residues. We also demonstrated that MoTyr shared a closer phylogenetic lineage with *N. crassa*. These results are consistent with the reported structural characteristics of fungal tyrosinase, which confirms that MGG_14598 encodes a tyrosinase protein. The MoTyr expression pattern was observed to be upregulated during the stalk formation and early stage of infection; these results indicate that MoTyr may be involved in the pathogenic development of *M. oryzae*.

In nature, *M. oryzae* mainly uses asexual spores, conidia, as a source of infection to complete its entire infection cycle. The normal development and formation of conidia is

an essential part of the pathogenicity of *M. oryzae* [57]. To understand whether MoTyr is involved in the formation and development of conidia in *M. oryzae*, we generated Δ MoTyr mutant strains by deleting the MoTyr gene in wild-type *M. oryzae* strain, Y34. The results showed that the conidia morphology was not different from that of the wild-type. Still, the number of conidia of the mutant strain was significantly reduced compared with the wild-type. In previous studies, researchers have cloned and identified many genes that control sporulation. For example, the conidia morphology of the deleted mutants of *CON1*, *CON2* and *CON4* genes related to sporulation was abnormal, and the ratio of sporulation to wild-type also decreased significantly [58]. Similarly, deletion of *MoSTU1*, *MoHOX2* and *MoCON7* genes can lead to abnormal conidia formation in *M. oryzae* [59].

The development of conidiophore stalks plays a key role in the normal formation of conidia. The deletion of MoTyr resulted in conidia decrease in the number of *M. oryzae*. To further understand whether the decrease of conidia was related to the abnormal formation of conidiophore stalks, we stained the conidiophores with lactate phenol cotton blue. Our results showed that the mutant formed fewer conidiophore stalks than the wild type. This result is the same as *COS1*, a conidiophore stalk-less1 gene; the deletion of *COS1* results in a complete loss of conidiophore stalks development, resulting in the inability to produce conidia in *M. oryzae* [60]. Our results are identical to the effect of the carbonic anhydrase (*CA1*) gene; the deletion of *CA1* resulted in a decrease in the number of conidiophore stalks and conidiation [61]. Furthermore, the deletion of glycogen synthase kinase (*GSK1*) in *M. oryzae* results in the complete loss of conidiophore stalks and conidiation [62]. These results indicate that the abnormal development of conidiophore stalks often affects the formation of conidia. But these results differ from the role of *HTF1*, as the deletion of *HTF1* blocked conidiation but not the development of conidiophore stalks in *M. oryzae* [63]. This result suggests that the formation of conidiophore stalks may not be directly regulated by *HTF1* but can affect conidia formation. However, in our study, the number of conidiophore stalks and conidia decreased in the MoTyr deletion mutants, indicating that the MoTyr may directly regulate the formation of conidiophore stalks and then regulate the normal development of conidia.

In fungi, melanin increases the fungal tolerance towards extreme environments, including radiation, oxidants, enzymatic lysis, extreme temperatures, toxic metals and ionizing radiation and host immune responses [24,47,64]. In *Pestalotiopsis fici*, the deletion of PfMAE led to increased UV sensitivity of spores [65]. At extreme temperatures (42–47 °C), *Streptomyces galbus* produces more melanin, which thickens its cell wall and protects it from heat damage [66]. In *C. neoformans*, melanin also buffers physical damage, such as cold temperatures and protects cells from intracellular and extracellular ice crystals [67]. In *M. oryzae*, *ALB1*, *RSY1*, and *BUF1* are essential for conidial resistance to UV exposure, oxidation and freezing damage: deletion of these genes inhibited conidial germination [24]. Comparable results were found in our study, where the deletion of MoTyr led to reduced melanin synthesis and inhibited conidial germination under UV and freezing stress.

Melanin is produced by many organisms, including pathogenic fungi, where it can play a role as an important virulence factor. The appressorium is a highly pigmented and thick-walled structure formed by *M. oryzae* during infection. It is a site of intense melanin production and an important intermediate organ in the host infected by *M. oryzae*. In the process of appressorium maturation, glycerol and other substances continue to accumulate in the appressorium up to 3.0 MPa, making its internal turgor constantly rise to about 8.0 MPa, providing enough internal pressure for it to penetrate the host cuticle cells [68]. Our study found that the appressorium of the Δ MoTyr mutant strains was more prone to collapse under different concentrations of glycerol and PEG. Like our study, appressorium turgor pressure was abnormal after MoSwi6 (an APSES family transcription factor) deletion under glycerol treatment, and most of the appressorium could not penetrate rice cells [69]. However, in the corn pathogen *Colletotrichum graminicola*, deletion of *CgPKS1* led to non-melanized cell walls but normal turgor pressure in its appressoria [70]. The abnormal synthesis of melanin leads to a low-integrity appressorium wall, which was

unable to produce high appressorium turgor to penetrate the plant [36]. In *M. oryzae*, MoCA1 participates in appressorium maturation and morphogenesis; it was found that the loss of the gene reduced melanin synthesis and infection ability [61]. C3HC type Zinc-finger protein (ZFC3) and deletion of this gene led to increased melanin synthesis and its ability to infect rice cells [71]. These results suggest that *M. oryzae* requires melanin for appressorial turgor. These results are similar to our study, where the loss of tyrosinase leads to a lower level of melanin synthesis and causes the appressorium to collapse more easily. Therefore the infection ability of mutant strains decreased significantly. Also, during the development of appressorium, melanin synthesis was blocked, and the normal turgor pressure could not be maintained, which resulted in a weakened penetration ability of the penetration peg.

Previous studies have shown that *M. oryzae* utilizes the DHN melanin pathway. In our study, we found that after the deletion of MoTyr, melanin synthesis in *M. oryzae* decreased significantly. To this end, we detected the expression levels of *ALB1*, *BUF1* and *RSY*, which are key genes involved in the melanin synthesis pathway of *M. oryzae*. The results showed that the expression level of *BUF1* and *RSY* was significantly decreased in mutant strains (Figure 6). However, whether tyrosinase is also involved in melanin synthesis in *M. oryzae* was unknown. Therefore, we hypothesized that the deletion of tyrosinase affects the expression of genes associated with the DHN melanin synthesis pathway, possibly because tyrosinase has a catalytic substrate in *M. oryzae*. However, this substrate may have a feedback regulatory relationship with the substrates of the DHN melanin synthesis pathway, which leads to a decrease in the expression level of genes related to the DHN melanin synthesis pathway.

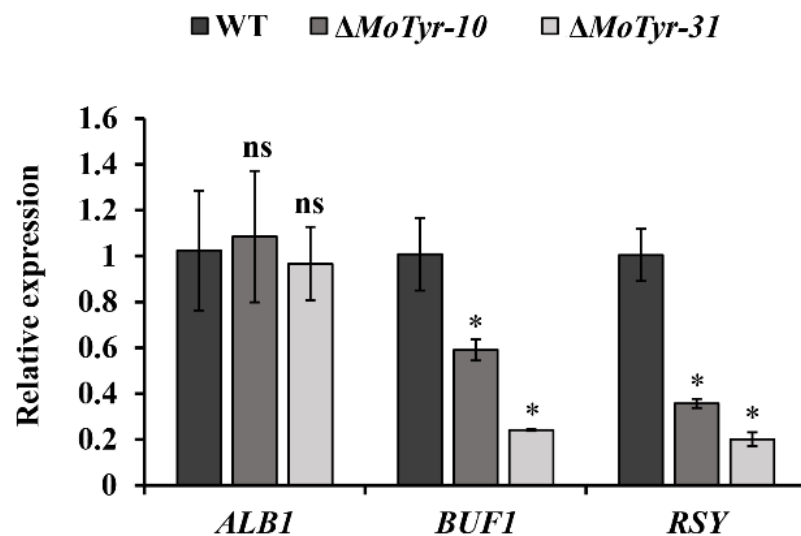


Figure 6. Expression analysis of melanin-related genes *ALB1*, *BUF1* and *RSY1*. Asterisks * represent a statistically significant difference of $p < 0.05$; ns represent not significant.

In conclusion, we demonstrate that MoTyr is required for conidiogenesis, appressorium development and melanin synthesis, which leads to the successful pathogenic development of *M. oryzae*. Tyrosinase is a rate-limiting enzyme involved in DOPA melanin synthesis, but the mechanism of its involvement in the DHN melanin synthesis pathway of *M. oryzae* remains unclear and needs further study.

Supplementary Materials: The following supporting information can be downloaded at: <https://www.mdpi.com/article/10.3390/jof9030311/s1>, Figure S1: Melanin synthesis pathway.title; Figure S2: Construction of vectors and verification of mutants; Figure S3: Growth characteristics of wild-type and Δ MoTyr mutant stains; Figure S4: Conidia germination and appressoria formation; Table S1: Primers used in this study.

Author Contributions: S.-H.Z. and X.F. designed the research and analyzed the data. P.Z., W.B., C.L., Y.H., Y.W. and Z.H. assisted in part of the experimental process. S.-H.Z. and X.F. wrote the manuscript. All authors have read and agreed to the published version of the manuscript.

Funding: This work was supported by the Natural Science Foundation of China (Grant Nos. 32172364, 31671972 to S.-H.Z. and 31670141 to Y.W.); the Special talent introduction of Shenyang Agricultural University of China (Grant No. 880420019 to S.-H.Z.).

Institutional Review Board Statement: Not applicable.

Informed Consent Statement: Not applicable.

Data Availability Statement: Not applicable.

Conflicts of Interest: The authors declare no conflict of interest.

References

1. Tran-Ly, A.N.; Reyes, C.; Schwarze, F.W.; Ribera, J. Microbial production of melanin and its various applications. *World J. Microbiol. Biotechnol.* **2020**, *36*, 170. [[CrossRef](#)] [[PubMed](#)]
2. Liu, R.; Meng, X.; Mo, C.; Wei, X.; Ma, A. Melanin of fungi: From classification to application. *World J. Microbiol. Biotechnol.* **2022**, *38*, 228. [[CrossRef](#)] [[PubMed](#)]
3. Smith, D.F.Q.; Casadevall, A. The role of melanin in fungal pathogenesis for animal hosts. In *Fungal Physiology and Immunopathogenesis*; Springer: Cham, Switzerland, 2019; pp. 1–30.
4. Emidio, C.P.E.E.; Urán, J.M.; Silva, B.R.L.S.; Dias, L.; Doprado, M.; Nosanchuk, J.D.; Tabora, C.P. Melanin as a virulence factor in different species of genus *Paracoccidioides*. *J. Fungi* **2020**, *6*, 291. [[CrossRef](#)]
5. Pal, A.K.; Gajjar, D.U.; Vasavada, A.R. DOPA and DHN pathway orchestrate melanin synthesis in *Aspergillus species*. *Med. Mycol.* **2014**, *52*, 10–18.
6. Butler, M.J.; Day, A.W. Fungal melanins: A review. *Can. J. Microbiol.* **1998**, *44*, 1115–1136. [[CrossRef](#)]
7. Strycker, B.D.; Han, Z.; Bahari, A.; Pham, T.; Lin, X.; Shaw, B.D.; Sokolov, A.V.; Scully, M.O. Raman characterization of fungal DHN and DOPA melanin biosynthesis pathways. *J. Fungi* **2021**, *7*, 841. [[CrossRef](#)] [[PubMed](#)]
8. Bell, A.A.; Wheeler, M.H. Biosynthesis and functions of fungal melanins. *Ann. Rev. Phytopathol.* **1986**, *24*, 411–451. [[CrossRef](#)]
9. Woloshuk, C.P.; Sisler, H.D. Tricyclazole, pyroquilon, tetrachlorophthalide, PCBA, coumarin and related compounds inhibit melanization and epidermal penetration by *Pyricularia oryzae*. *J. Pestic. Sci. Int. Ed.* **1982**, *7*, 161–166. [[CrossRef](#)]
10. Takano, Y.; Kubo, Y.; Kuroda, L.; Furusawa, I. Temporal transcriptional pattern of three melanin biosynthesis genes, *PKS1*, *SCD1* and *THR1*, in appressorium-differentiating and nondifferentiating conidia of *Colletotrichum lagenarium*. *Appl. Environ. Microbiol.* **1997**, *63*, 351–354. [[CrossRef](#)] [[PubMed](#)]
11. Kubo, Y.; Takano, Y.; Endo, N.; Yasuda, N.; Tajima, S.; Furusawa, I. Cloning and structural analysis of the melanin biosynthesis gene *SCD1* encoding scytalone dehydratase in *Colletotrichum lagenarium*. *Appl. Environ. Microbiol.* **1996**, *61*(62), 4340–4344. [[CrossRef](#)] [[PubMed](#)]
12. Jiang, H.; Chi, Z.; Liu, G.L.; Hu, Z.; Zhao, S.Z.; Chi, Z.M. Melanin biosynthesis in the desert-derived *Aureobasidium melanogenum* XJ5-1 is controlled mainly by the CWI signal pathway via a transcriptional activator Cmr1. *Curr. Genet.* **2020**, *66*, 173–185. [[CrossRef](#)]
13. Casadevall, A. Melanin, melanin and composition in *Cryptococcus neoformans*. *Infect. Immun.* **1996**, *64*, 2420–2424.
14. Nosanchuk, J.D.; Gomez, B.L.; Youngchim, S.; Diez, S.; Aisen, P.; Zancope-Oliveira, R.; Restrepo, A.; Casadevall, A.; Hamilton, A.J. *Histoplasma capsulatum* synthesizes melanin-like pigments in vitro and during mammalian infection. *Infect. Immun.* **2002**, *70*, 5124–5131. [[CrossRef](#)]
15. Morris-Jones, R.; Gomez, B.L.; Diez, S.; Uran, M.; Morris-Jones, S.D.; Casadevall, A.; Nosanchuk, J.D.; Hamilton, A.J. Synthesis of melanin pigment by *Candida albicans* in vitro and during infection. *Infect. Immun.* **2005**, *73*, 6147–6150. [[CrossRef](#)] [[PubMed](#)]
16. Singh, S.; Nimse, S.B.; Mathew, D.E.; Dhimmar, A.; Sahastrabudhe, H.; Gajjar, A.; Ghadge, V.A.; Kumar, P.; Shinde, P.B. Microbial melanin: Recent advances in biosynthesis, extraction, characterization, and applications. *Biotechnol. Adv.* **2021**, *53*, 107773. [[CrossRef](#)] [[PubMed](#)]
17. Chumley, F.; Valent, B. Genetic analysis of melanin-deficient, nonpathogenic mutants of *Magnaporthe grisea*. *Mol. Plant Microbe Interact.* **1990**, *3*, 135–143. [[CrossRef](#)]
18. Kihara, J.; Moriwaki, A.; Ueno, M.; Tokunaga, T.; Arase, S.; Honda, Y. Cloning, functional analysis and expression of a scytalone dehydratase gene (*SCD1*) involved in melanin biosynthesis of the phytopathogenic fungus *Bipolaris oryzae*. *Curr. Genet.* **2004**, *45*, 197–204. [[CrossRef](#)] [[PubMed](#)]
19. Skory, C.D.; Chang, P.K.; Cary, J.; Linz, J.E. Isolation and characterization of a gene from *Aspergillus parasiticus* associated with the conversion of versicolorin A to sterigmatocystin in aflatoxin biosynthesis. *Appl. Environ. Microbiol.* **1992**, *58*, 3527–3537. [[CrossRef](#)]
20. Wang, X.; Lu, D.; Tian, C. Analysis of melanin biosynthesis in the plant pathogenic fungus *Colletotrichum gloeosporioides*. *Fungal Biol.* **2021**, *125*, 679–692. [[CrossRef](#)] [[PubMed](#)]

21. Romero-Martinez, R.; Wheeler, M.; Guerrero-Plata, A.; Rico, G.; Torres-Guerrero, H. Biosynthesis and functions of melanin in *Sporothrix schenckii*. *Infect. Immun.* **2000**, *68*, 3696–3703. [[CrossRef](#)] [[PubMed](#)]
22. Ma, S.; Cao, K.; Liu, N.; Meng, C.; Cao, Z.; Dai, D.; Jia, H.; Zang, J.; Li, Z.; Hao, Z.; et al. The *StLAC2* gene is required for cell wall integrity, DHN-melanin synthesis and the pathogenicity of *Setosphaeria turcica*. *Fungal Biol.* **2017**, *121*, 589–601. [[CrossRef](#)] [[PubMed](#)]
23. Oh, Y.; Donofrio, N.; Pan, H.Q.; Coughlan, S.; Brown, D.E.; Meng, S.W.; Mitchell, T.; Dean, R.A. Transcriptome analysis reveals new insight into appressorium formation and function in the rice blast fungus *Magnaporthe oryzae*. *Genome Biol.* **2008**, *9*, R85. [[CrossRef](#)] [[PubMed](#)]
24. Zhu, S.; Yan, Y.; Qu, Y.; Wang, J.; Feng, X.; Liu, X.; Lin, F.; Lu, J.-P. Role refinement of melanin synthesis genes by gene knockout reveals their functional diversity in *Pyricularia oryzae* strains. *Microbiol. Res.* **2021**, *242*, 126620. [[CrossRef](#)]
25. Langfelder, K.; Streibel, M.; Jahn, B.; Haase, G.; Brakhage, A.A. Biosynthesis of fungal melanins and their importance for human pathogenic fungi. *Fungal Genet. Biol.* **2003**, *38*, 143–158. [[CrossRef](#)] [[PubMed](#)]
26. Pavan, M.E.; López, N.I.; Pettinari, M.J. Melanin biosynthesis in bacteria, regulation and production perspectives. *Appl. Microbiol. Biotechnol.* **2020**, *104*, 1357–1370. [[CrossRef](#)]
27. Ismaya, W.T.; Rozeboom, H.J.; Weijn, A.; Mes, J.J.; Fusetti, F.; Wichers, H.J.; Dijkstra, B.W. Crystal structure of *Agaricus bisporus* mushroom tyrosinase: Identity of the tetramer subunits and interaction with tropolone. *Biochemistry* **2011**, *50*, 5477–5486. [[CrossRef](#)] [[PubMed](#)]
28. Goldfeder, M.; Egozy, M.; Shuster Ben-Yosef, V.; Adir, N.; Fishman, A. Changes in tyrosinase specificity by ionic liquids and sodium dodecyl sulfate. *Appl. Microbiol. Biotechnol.* **2013**, *97*, 1953–1961. [[CrossRef](#)] [[PubMed](#)]
29. Pretzler, M.; Bijelic, A.; Rompel, A. Heterologous expression and characterization of functional mushroom tyrosinase (AbPPO4). *Sci. Rep.* **2017**, *7*, 1810. [[CrossRef](#)]
30. Zolghadri, S.; Bahrami, A.; Hassan Khan, M.T.; Munoz-Munoz, J.; Garcia-Molina, F.; Garcia-Canovas, F.; Saboury, A.A. A comprehensive review on tyrosinase inhibitors. *J. Enzym. Inhib. Med. Chem.* **2019**, *34*, 279–309. [[CrossRef](#)]
31. Cabezudo, I.; Ramallo, I.A.; Alonso, V.L.; Furlan, R.L. Effect directed synthesis of a new tyrosinase inhibitor with anti-browning activity. *Food Chem.* **2021**, *341*, 128232. [[CrossRef](#)]
32. Rao, A.; Pimprikar, P.; Bendigiri, C.; Kumar, A.R.; Zinjarde, S. Cloning and expression of a tyrosinase from *Aspergillus oryzae* in *Yarrowia lipolytica*: Application in L-DOPA biotransformation. *Appl. Microbiol. Biotechnol.* **2011**, *92*, 951–959. [[CrossRef](#)] [[PubMed](#)]
33. Li, T.; Zhang, N.; Yan, S.; Jiang, S.; Yin, H. A novel tyrosinase from *Armillaria ostoyae* with comparable monophenolase and diphenolase activities suffers substrate inhibition. *Appl. Microbiol. Biotechnol.* **2021**, *87*, e00275-21. [[CrossRef](#)] [[PubMed](#)]
34. Chen, Q.; Liu, F.; Kong, Q.; Wu, Y.; He, Y.; Sang, H. Fungal melanin-induced metabolic reprogramming in macrophages is crucial for inflammation. *J. Med. Mycol.* **2023**, 101359. [[CrossRef](#)] [[PubMed](#)]
35. Boddy, L. Pathogens of Autotrophs. *Fungi* **2016**, *3*, 245–292.
36. Gupta, L.; Vermani, M.; Kaur Ahluwalia, S.; Vijayaraghavan, P. Molecular virulence determinants of *Magnaporthe oryzae*: Disease pathogenesis and recent interventions for disease management in rice plant. *Mycology* **2021**, *12*, 174–187. [[CrossRef](#)]
37. Batool, W.; Shabbir, A.; Lin, L.; Chen, X.; An, Q.; He, X.; Pan, S.; Chen, S.; Chen, Q.; Wang, Z.; et al. Translation initiation factor eIF4E positively modulates conidiogenesis, appressorium formation, host invasion and stress homeostasis in the filamentous fungus *Magnaporthe oryzae*. *Front. Plant Sci.* **2021**, *12*, 646343. [[CrossRef](#)]
38. Batool, W.; Liu, C.; Fan, X.; Zhang, P.; Hu, Y.; Wei, Y.; Zhang, S.-H. AGC/AKT protein kinase SCH9 is critical to pathogenic development and overwintering survival in *Magnaporthe oryzae*. *J. Fungi* **2022**, *8*, 810. [[CrossRef](#)]
39. Abdul, W.; Aliyu, S.R.; Lin, L.; Sekete, M.; Chen, X.; Otieno, F.J.; Yang, T.; Lin, Y.H.; Norvienyeku, J.; Wang, Z.-H. Family-four aldehyde dehydrogenases play an indispensable role in the pathogenesis of *Magnaporthe oryzae*. *Front. Plant Sci.* **2018**, *9*, 980. [[CrossRef](#)] [[PubMed](#)]
40. Dang, Y.; Wei, Y.; Zhang, P.; Liu, X.; Li, X.; Wang, S.; Liang, H.; Zhang, S.-H. The bicarbonate transporter (MoAE4) localized on both cytomembrane and tonoplast promotes pathogenesis in *Magnaporthe oryzae*. *J. Fungi* **2021**, *7*, 955. [[CrossRef](#)] [[PubMed](#)]
41. Tang, W.; Jiang, H.; Zheng, Q.; Chen, X.; Wang, R.; Yang, S.; Zhao, G.; Liu, J.; Norvienyeku, J.; Wang, Z. Isopropylmalate isomerase MoLeu1 orchestrates leucine biosynthesis, fungal development, and pathogenicity in *Magnaporthe oryzae*. *Appl. Microbiol. Biotechnol.* **2019**, *103*, 327–337. [[CrossRef](#)]
42. Nakamura, M.; Nakajima, T.; Ohba, Y.; Yamauchi, S.; Lee, B.-R.; Ichishima, E. Identification of copper ligands in *Aspergillus oryzae* tyrosinase by site-directed mutagenesis. *Biochem. J.* **2000**, *350*, 537–545. [[CrossRef](#)]
43. Kanteev, M.; Goldfeder, M.; Chojnacki, M.; Adir, N.; Fishman, A. The mechanism of copper uptake by tyrosinase from *Bacillus megaterium*. *J. Biol. Inorg. Chem.* **2013**, *18*, 895–903. [[CrossRef](#)] [[PubMed](#)]
44. Noh, H.; Lee, S.; Jo, H.J.; Choi, H.W.; Hong, S.; Kong, K. Histidine residues at the copper-binding site in human tyrosinase are essential for its catalytic activities. *J. Enzym. Inhib. Med. Chem.* **2020**, *35*, 726–732. [[CrossRef](#)] [[PubMed](#)]
45. Setaluri, V. Sorting and targeting of melanosomal membrane proteins: Signals, pathways, and mechanisms. *Pigment. Cell Res.* **2000**, *13*, 128–134. [[CrossRef](#)]
46. Decker, H.; Schweikardt, T.; Nillius, D.; Salzbrunn, U.; Jaenicke, E.; Tucek, F. Similar enzyme activation and catalysis in hemocyanins and tyrosinases. *Gene* **2007**, *398*, 183–191. [[CrossRef](#)] [[PubMed](#)]
47. Cordero, R.J.; Casadevall, A. Melanin. *Curr. Biol.* **2020**, *30*, 142–143. [[CrossRef](#)] [[PubMed](#)]

48. Cordero, R.J.; Casadevall, A. Functions of fungal melanin beyond virulence. *Fungal Biol. Rev.* **2017**, *31*, 99–112. [[CrossRef](#)] [[PubMed](#)]
49. Fernandez, C.W.; Koide, R.T. The function of melanin in the ectomycorrhizal fungus *Cenococcum geophilum* under water stress. *Fungal Ecol.* **2013**, *6*, 479–486. [[CrossRef](#)]
50. Rangel Montoya, E.A.; Paolinelli, M.; Rolshausen, P.; Hernandez Martinez, R. The role of melanin in the grapevine trunk disease pathogen *Lasiodiplodia gilanensis*. *Phytopathol. Mediterr.* **2020**, *59*, 549–563.
51. Kampatsikas, I.; Bijelic, A.; Pretzler, M.; Rompel, A. Three recombinantly expressed apple tyrosinases suggest the amino acids responsible for mono-versus diphenolase activity in plant polyphenol oxidases. *Sci. Rep.* **2017**, *7*, 8860. [[CrossRef](#)] [[PubMed](#)]
52. Neupane, N.; Bhusal, K. A review of blast disease of rice in Nepal. *J. Plant Pathol. Microbiol.* **2021**, *11*, 528.
53. Talbot, N.J. On the trail of a cereal killer: Exploring the biology of *Magnaporthe grisea*. *Annu. Rev. Microbiol.* **2003**, *57*, 177–202. [[CrossRef](#)]
54. Pennisi, E. Armed and dangerous. *Science* **2010**, *327*, 804–805.
55. Butler, M.J.; Day, A.W.; Henson, J.M.; Money, N.P. Pathogenic properties of fungal melanins. *Mycologia* **2001**, *93*, 1–8. [[CrossRef](#)]
56. Nosanchuk, J.D.; Casadevall, A. The contribution of melanin to microbial pathogenesis. *Cell. Microbiol.* **2003**, *5*, 203–223. [[CrossRef](#)]
57. Shi, H.; Meng, S.; Qiu, J.; Wang, C.; Shu, Y.; Luo, C.; Kou, Y. MoWhi2 regulates appressorium formation and pathogenicity via the MoTor signalling pathway in *Magnaporthe oryzae*. *Mol. Plant Pathol.* **2021**, *22*, 969–983. [[CrossRef](#)] [[PubMed](#)]
58. Shi, Z.; Leung, H. Genetic analysis of sporulation in *Magnaporthe grisea* by chemical and insertional mutagenesis. *Mol. Plant Microbe Interact.* **1995**, *8*, 949–959. [[CrossRef](#)]
59. Yang, J.; Zhao, X.; Sun, J.; Kang, Z.; Ding, S.; Xu, J.R.; Peng, Y.L. A novel protein Com1 is required for normal conidium morphology and full virulence in *Magnaporthe oryzae*. *Mol. Plant Microbe Interact.* **2010**, *23*, 112–123. [[CrossRef](#)] [[PubMed](#)]
60. Zhou, Z.; Li, G.; Lin, C.; He, C. Conidiophore stalk-less1 encodes a putative zinc-finger protein involved in the early stage of conidiation and mycelial infection in *Magnaporthe oryzae*. *Mol. Plant Microbe Interact.* **2009**, *22*, 402–410. [[CrossRef](#)]
61. Dang, Y.; Wei, Y.; Batool, W.; Sun, X.; Li, X.; Zhang, S.-H. Contribution of the mitochondrial carbonic anhydrase (MoCA1) to conidiogenesis and pathogenesis in *Magnaporthe oryzae*. *Front. Microbiol.* **2022**, *13*, 845570. [[CrossRef](#)] [[PubMed](#)]
62. Zhou, T.; Dagdas, Y.F.; Zhu, X.; Zheng, S.; Chen, L.; Cartwright, Z.; Talbot, N.J.; Wang, Z. The glycogen synthase kinase MoGsk1, regulated by Mps1 MAP kinase, is required for fungal development and pathogenicity in *Magnaporthe oryzae*. *Sci. Rep.* **2017**, *7*, 945. [[CrossRef](#)] [[PubMed](#)]
63. Liu, W.; Xie, S.; Zhao, X.; Chen, X.; Zheng, W.; Lu, G.; Xu, J.; Wang, Z. A homeobox gene is essential for conidiogenesis of the rice blast fungus *Magnaporthe oryzae*. *Mol. Plant Microbe Interact.* **2010**, *23*, 366–375. [[CrossRef](#)] [[PubMed](#)]
64. Zhong, J.; Frases, S.; Wang, H.; Casadevall, A.; Stark, R.E. Following fungal melanin biosynthesis with solid-state NMR: Biopolymer molecular structures and possible connections to cell-wall polysaccharides. *Biochemistry* **2008**, *47*, 4701–4710. [[CrossRef](#)]
65. Zhang, P.; Wang, X.N.; Fan, A.L.; Zheng, Y.J.; Liu, X.Z.; Wang, S.H.; Zou, H.X.; Oakley, B.R.; Keller, N.P.; Yin, W.B. A cryptic pigment biosynthetic pathway uncovered by heterologous expression is essential for conidial development in *Pestalotiopsis fici*. *Mol. Microbiol.* **2017**, *105*, 469–483. [[CrossRef](#)] [[PubMed](#)]
66. Filippova, S.N.; Kuznetsov, V.D.; Zaslavskaya, P.L. Production of melanins by *Streptomyces galbus* as a response to the elevated temperature of its cultivation and melanin localization. *Mikrobiologiya* **1987**, *56*, 710–712.
67. Rosas, A.L.; Casadevall, A. Melanization affects susceptibility of *Cryptococcus neoformans* to heat and cold. *FEMS Microbiol. Lett.* **1997**, *153*, 265–272. [[CrossRef](#)]
68. Foster, A.J.; Ryder, L.S.; Kershaw, M.J.; Talbot, N.J. The role of glycerol in the pathogenic lifestyle of the rice blast fungus *Magnaporthe oryzae*. *Environ. Microbiol.* **2017**, *19*, 1008–1016. [[CrossRef](#)]
69. Qi, Z.; Wang, Q.I.; Dou, X.; Wang, W.; Zhao, Q.; Lv, R.; Zhang, H.; Zheng, X.; Wang, P.; Zhang, Z. MoSwi6, an APSES family transcription factor, interacts with MoMps1 and is required for hyphal and conidial morphogenesis, appressorial function and pathogenicity of *Magnaporthe oryzae*. *Mol. Plant Pathol.* **2012**, *13*, 677–689. [[CrossRef](#)]
70. Ludwig, N.; Lohrer, M.; Hempel, M.; Mathea, S.; Schliebner, I.; Menzel, M.; Kiesow, A.; Schaffrath, U.; Deising, H.B.; Horbach, R. Melanin is not required for turgor generation but enhances cell-wall rigidity in appressoria of the corn pathogen *Colletotrichum graminicola*. *Mol. Plant Microbe Interact.* **2014**, *27*, 315–327. [[CrossRef](#)]
71. Liu, S.; Wei, Y.; Zhang, S.-H. The C3HC type zinc-finger protein (ZFC3) interacting with Lon/MAP1 is important for mitochondrial gene regulation, infection hypha development and longevity of *Magnaporthe oryzae*. *BMC Microbiol.* **2020**, *20*, 23. [[CrossRef](#)]

Disclaimer/Publisher’s Note: The statements, opinions and data contained in all publications are solely those of the individual author(s) and contributor(s) and not of MDPI and/or the editor(s). MDPI and/or the editor(s) disclaim responsibility for any injury to people or property resulting from any ideas, methods, instructions or products referred to in the content.